

# Classification of Imagined Motor Tasks for BCI

Plamen Doynov, Jesse Sherwood, Reza Derakhshani  
School of Computing and Engineering  
University of Missouri – Kansas City  
Kansas City, MO 64110 USA

**Abstract-** Electroencephalography (EEG) is a well developed technique used in many clinical and research applications. Continuous improvements on quality of scalp electrodes and front-end amplifiers, and data processing and storage have elevated EEG to a standard non-invasive method for monitoring many brain functions. EEG can also provide a new means for sending messages to the external world which is commonly known as a Brain-Computer Interface (BCI). This paper describes different feature extraction techniques for classification of recorded EEG signals. Time and frequency processing of multichannel EEG recordings during four *a priori* known mental tasks is presented. The four tasks include imagining the movement of an arm or a leg without the execution of the actual motion. During the recording sessions, the imagined movements are separated with intervals of subject relaxation. Different methods were used for feature extraction and classification of the EEG signals as a base for BCI. The results demonstrate that signals from an untrained subject can be classified successfully. The algorithms can be used to establish a real-time direct connection between mental task activity and external communication. In this regard we view the possibility for extending the neuroplasticity of the brain toward direct control of specifically designed external devices.

**Keywords:** Brain-computer interface, Imagined motor movements, Electro-encephalography, Signal Processing

## I INTRODUCTION

Electroencephalographic (EEG) signals originate from the cerebral pyramidal cells [1] and can be evoked by auditory [2], verbal [3], visual, and motor activities [4, 5]; as well as different emotions [6]. Digital processing of EEG signals for Brain-Computer Interfacing (or BCI) has received extensive attention in recent years [7, 8]. Unfortunately, EEG signals are contaminated by various artifacts such as the nonlinear, low pass filtering of the skull and “the chatter” from other brain circuits not targeted by a specific

BCI application, and thus need significant preprocessing [7]. The recent developments in understanding the functionality of the brain, the ever increasing computational power and lower cost and form factor of EEG-processing hardware have created new opportunities for assistive technologies such as BCI to meet the specific needs of patients with severe neural and muscular disorders (amyotrophic lateral sclerosis, for example.) In fact, BCI might be the only communication channel for “locked-in” patients.

EEG can be monitored and recorded using either external (non-invasive) and cranially implanted (invasive) electrodes. Each one of these modalities has its advantages and associated difficulties and limitations. Given the rich but noisy information contents of EEG signals, robust preprocessing and feature extraction algorithms are essential. The inherent low signal to noise ratio (SNR) of the non-invasively recorded EEGs, their low spatial resolution, as well as their short and long term non-stationary characters need to be addressed with proper preprocessing, feature extraction, and classification. Among the aforementioned obstacles, development of robust algorithms to accommodate the ever changing dynamics of the brain could be arguably the most challenging, as a BCI classifier trained on a subject may not behave similarly on the same subject after a few days [7]. The spatial distribution of EEG patterns, as well as their spectral characteristics, may also change from day to day [9].

BCIs be designed and implemented in many different ways. From a neurophysiologic perspective, BCI could be based on single (e.g. on/off operations) or multiple mental tasks (e.g. for operating a wheelchair). Regarding the choice of features, there are many options. For instance, for frequency-based features, one can use the ratios of the well established frequency bands such as delta (0.5 – 4 Hz), theta (4 -8 Hz), alpha (8 – 13 Hz), and beta (13 – 30 Hz). Other feature set options include time domain and joint time-frequency domain feature sets.

An imagined motor task can be defined as an intentional thought process with a predefined limb movement goal. The imagined motor tasks are performed within a recording

session in accordance with a protocol. Such protocol also provides a consistent basis for comparison between recording sessions, and usually includes a relaxation period between consecutive imagined tasks. Here we present the study of independent BCI, where intentional thoughts as defined above, in contrast to normal pathways of the brain, are used as an input stimulus for generation the brain activity.

Neuroplasticity is used to describe the changes of the brain that occur in response to experience. For a BCI, neuroplasticity can be viewed as the development and improvement of the subject's cognitive skills to navigate a particular BCI more successfully, which may occur as a result of biofeedback in long term usage. This phenomenon is beyond the scope of the presented study due to the short-term nature of our data collection.

#### A. Methods

EEG electrodes for this study were arranged over that scalp in accordance with the international 10-20 system. The 10-20 system uses a letter code for electrode locations where A stands for Ear lobe, C for central, Pg for nasopharyngeal, P for parietal, F for frontal, Fp for frontal polar, and O for occipital locations of the cranium.

The data used for this study were acquired from an untrained subject. We realize the limitations of this data set and its expansion is a focus of the ongoing study. The recording process was navigated by providing the subject with visual cues in form of simple text messages on a LCD screen. A total of 21 channels (including one ground electrode) were recorded using the NeuroPulse™ Systems' MS-24R QEEG system and the ECI Electro-Cap CS-2000-L electrode system. To insure a low impedance of the electrode scalp contact, each electrode cavity was filled with ECI Electro-gel™. Recordings were performed in a quiet lab with natural ambient light. Each recording session lasted 90 seconds and consisted of four 10-second imagined motor tasks separated with a subject relaxation of equal duration. More specifically, each session started with a 10 second relaxation period followed by intervals of 10 seconds during which the subject imagined moving his right arm (without any actual physical movements). After a consecutive 10 seconds relaxation, a second EEG of imagined movement of the left arm was recorded. The third mental task was movement of the right leg, followed by another relaxation period, imagined movement of the left leg, and a final relaxation. A total of five such sessions were recorded. The subject was allowed an extended resting period between each session.

The subject was restraining from eye movements during the mental tasks in order to avoid ocular EEG artifacts. Twenty channels were actively recorded. The first nineteen channels were connected to electrodes positioned firmly on the scalp using the aforementioned electro-cap and 10-20 electrode placement system. The 20<sup>th</sup> channel was connected from the ear-lobe (A1/A2) reference electrode to the linked b-channel input of the recording front-end preamplifier.

The recording was at a 256 Hz sampling rate and under the control of a desktop computer. The amplifier front-end incorporates two fourth-order Sallen-Key active filters with a 48 dB roll-off per octave and a 1.5 Hz – 34 Hz frequency pass band. Additional filtering was applied to further improve the 60 Hz rejection. The recorded data was preprocessed by removing the first and last second from each recorded imagined task. This produced raw recorded sessions with 8 seconds duration per imagined task, for a total of 2048 samples per imagined movement. Additionally, the data was preprocessed by displaying the channels of interest and manually removing the artifacts from unwanted ocular movement and electrode artifacts, as determined from (visual inspection). The onsets of artifacts were chosen as close to zero crossing as possible. Furthermore, these cut-off points were chosen so that their slopes would match, if possible, in order to avoid introduction of artificial changes of direction in the recorded signal. One needs to use automated artifact removal algorithms for larger datasets. However, for our small dataset, this simple manual process was deemed to be adequate.

After artifact removal, the data was filtered in MATLAB™. We used a low-pass elliptic filter with the following specifications: order of 10, pass frequency  $f_p$  of 50 Hz, stop frequency  $f_s$  of 60 Hz, and stop band attenuation of 60 dB. Additionally, a large Laplacian spatial filter was used to accentuate the localization of the EEG channel of interest ( $C_3$ ) on the motor cortex (spatial high-pass filtering). The  $C_3$  channel was used as the active channel for all sessions. Its four surrounding electrodes, namely channels 4 ( $F_3$ ), 10 ( $C_z$ ), 14 ( $P_3$ ), and 8 ( $T_3$ ), were averaged and used as a ground. The average ground signal was subtracted from the active electrode channel, or  $C_3 - \frac{1}{4}(F_3 + C_z + P_3 + T_3)$ , to implement the earlier-mentioned large Laplacian spatial filtering.

The preprocessing resulted in a total of 20 records (five separate sessions, four mental tasks per session). The process of feature extraction and classification in this study was guided by maximum linear separation as given by the Fisher linear discriminant classifier [10]. That is, the lower

the misclassification and intra-class variance and the higher inter-class distance, the higher the figure of merit. We conjecture that the deficiencies in the presented results are at least partially due to the limited size of our dataset. From the available five sessions, three were used for classifier design, one for validation, and one for performance evaluation (verification or testing). Once again one needs to view the following results in the light of the limitations set forth by the small size of our study data set.

### B. Time-domain Feature Extraction

For time-domain feature extraction, we used MATLAB<sup>TM</sup> function  $A = \text{LPC}(X, N)$  to obtain linear predictive coefficients of the EEG signals. Using this function we find the coefficients,  $A = [1 \ A(2) \ \dots \ A(N+1)]$ , of an autoregressive predictive model of the EEG signal  $X(n)$ , by minimizing

$$\text{err}(n) = X(n) - X_p(n) \quad (1)$$

Where

$$X_p(n) = \sum_{i=1}^N A(i+1)X(n-i) \quad (2)$$

The Fisher Linear Discriminant of the above LPC features was then used to calculate the separation between the four classes (imagined movements of right and left arm, right and left leg.) The Fisher's Linear Discriminant is based on linear projection of high-dimensional data for maximum linear classifiability. More specifically, for a two-class problem, it selects linear projection weight vector ( $w$ ) so to maximize inter-class vs. intra-class distance  $J(w)$ , where  $m_1$  and  $m_2$  represent the sample means for each class, and  $s_1$  and  $s_2$  represent their sample variances [10]

$$J(w) = \frac{(m_1 - m_2)^2}{s_1^2 + s_2^2} \quad (3)$$

Given the dichotomous nature of the above Fisher Discriminant, we divided our data into target-class and non-target-class groups. To clarify this terminology let us label the four mental tasks as RH, LH, RL, and LL for right hand, left hand, right leg, and left leg imagined movements, respectively. With this naming convention, the RH *target-class* (class  $C_1$ ) consists of RH data samples. The RH *non-target-class* (class  $C_2$ ) consists of LH, RL, and LL data samples. Fisher's discriminant computes the scalar linear projection of each class on a vector according to Eq. (3). We used formula (4) to find the projected *target-class* and *non-target-class* for each of the four mental tasks. Figure 1

presents such separation of the four classes when 5<sup>th</sup>-order LPC was used.

$$y(t) = w^T x(t) = \sum_{i=0}^n w_i x_i(t) \quad (4)$$

Note the legend used in Figure 1 to separate the validation and the and test results.

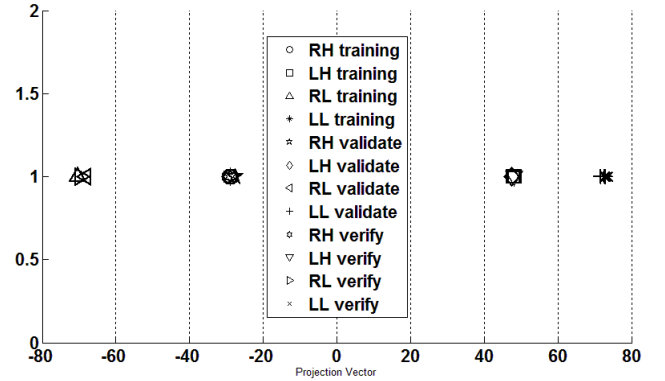


Fig. 1. Fisher Discriminant projection displays the class separation based on a 5<sup>th</sup> order AR features.

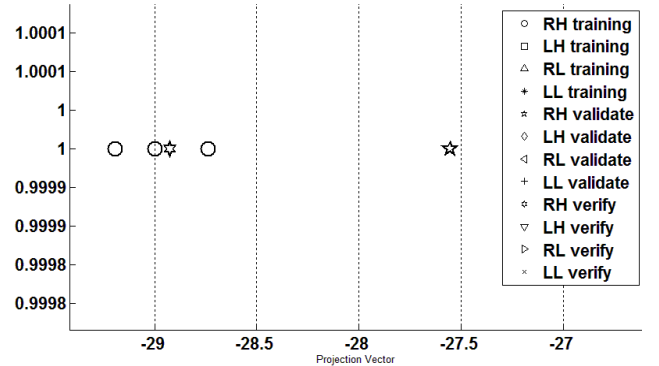


Fig. 2. Expanded area from Figure 1 plots showing RH class.

Figure 2 zooms into the RH class projection of Figure 1. Notice the close intra-class clustering. To summarize, Figure 1 shows 100% separation (100% correct classification) for all four classes (the larger the separation, the better). Figure 2 shows the close proximity of the projections from BCI commands within the RH class (lower variance is better).

### C. Frequency Domain Feature Extraction

The presence of distinct salient frequency bands in EEG recordings is well known, and thus the spectral energy of standard frequency bins has been used for diagnostic and evaluation purposes [11]. These frequency bands are known

as delta (0.5 – 4 Hz), theta (4 -8 Hz), alpha (8 – 13 Hz), and beta (13 – 30 Hz). Figure 3 displays the power spectral distribution for the first session of our dataset.

MATLAB™’s Welch spectrum estimator with Kaiser windowing was used for power spectral density estimation (PSD) of our EEG data. Visual examination of the PSD resulted in observing the frequency bands in which the functions differ from each other. We selected frequency bins for frequency-domain feature extraction as follows: The 0-50 Hz range was divided into nine bins with the following frequency boundaries in Hz:(1-7), (8-12),

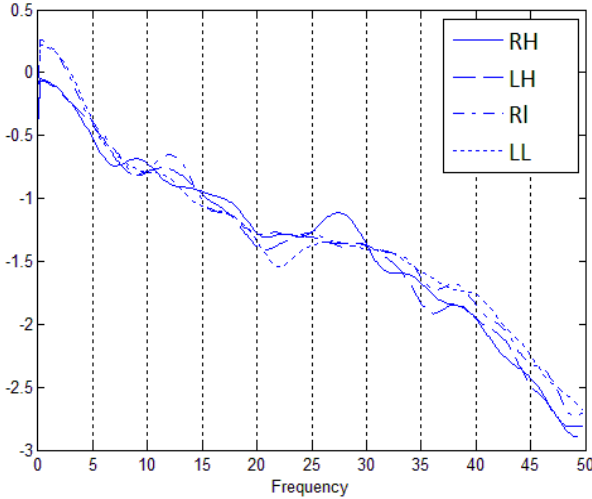


Fig. 3. Semi-log plots of session 1 EEG PSD

(13-17), (18-22), (23-29), (30-34), (35-29), (40-44), and (45-50). The *target-class* and *non-target-class* were formed for the four different mental tasks in the same way as for the time domain processing. The features for the *target-class* were selected as the area under the PSD curve for the aforementioned frequency bins. Finally, using the Fisher’s linear discriminant projection, the features were classified. The classification results are presented in Figure 4.

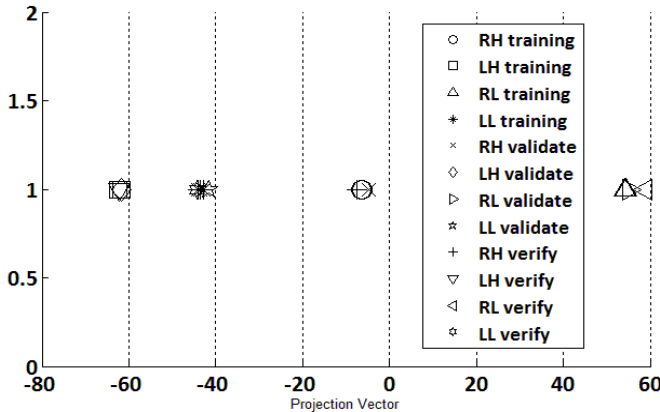


Fig. 4. Frequency-based classification results using PSD sub-bands and Fisher linear discriminant projection

This technique also resulted in 100% separation for the four classes with sufficient interclass distances, as can be seen from the above figure. The clustering of the data for each of the five recording sessions is also good.

#### D. Time and Frequency Domain Feature Extraction

Feature extraction can also be based on a combination of the above time and frequency feature sets, which is also known as fusion or multimodality at the feature level [12]. Given adequate training data, this approach can further enhance the performance of the classifier by increasing the dimensionality of the feature space. Such combination of the features can be achieved by simply concatenating the features that were calculated separately in time and in frequency domains. Alternatively, feature extraction algorithms can directly extract correlated time-frequency features. One such approach is using the spectrogram of the EEG.

Figure 5 shows the classification based on joint time and frequency domain feature extraction and Fisher linear projection. In this case features extracted in time domain were concatenated with features obtained in frequency domain. Used together they resulted in classification with significantly better cluster separation. The closest distance for time domain separation is about 50 relative units. For frequency domain the closest clusters are about 20 relative units. As Fig. 5 shows, the concatenation of the features from time and frequency domains result in a 100% successful classification and better than  $10^3$  vector projection separation.

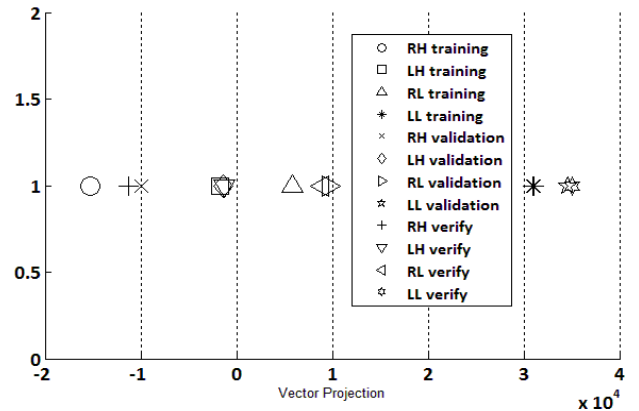


Fig. 5. Fisher Discriminant Projection of class separation based on joint time and frequency features.

#### E. Wavelet based Feature Extraction

It has been shown that taking the discrete wavelet transform of a function is equivalent to filtering a signal by a bank of constant-Q filters, the non-overlapping bandwidths of which differ by an octave [13].

For the wavelet decomposition, the EEG signals were first filtered with a low-pass, equiripple filter with order 8, pass frequency  $f_p$  of 40 Hz, stop frequency  $f_s$  of 50 Hz, and attenuation slope of 60 dB. The wavelet feature extraction was based on a one-dimensional Coiflet 5 wavelet decomposition. The MATLAB™ “wavedec” function was used to obtain the results. ‘Coif5’ is the MATLAB™ implementation of the Coifman 5<sup>th</sup>-order wavelet. This wavelet is generally characterized as a family of compactly supported wavelets with the highest number of vanishing moments for both scaling and wavelet functions for a given support width, as compared to other wavelet families [14]. All EEG signals were processed with the discrete wavelet transform which yielded a series of 8 filter coefficients. An input signal  $x(t)$  can be approximated by a series of wavelet basis functions  $\Psi_{n,k}(t)$ , *i.e.*

$$x(t) = \sum_{n=-\infty}^{\infty} \sum_{k=-\infty}^{\infty} d_{k,n} \Psi_{n,k}(t) \quad (5)$$

The wavelets are defined as

$$\Psi_{n,k}(t) = 2^{-\frac{n}{2}} \Psi(2^{-n}t - k) \quad (6)$$

Note that  $\Psi(2^{-n}t)$  represents a dilated or spread out version of  $\Psi(t)$ , as by increasing  $n$  (scale factor), the function becomes more spread out.  $\Psi(t - k)$  represents a time-shifted version of the function [14]. The wavelet decomposition produces the wavelet filter coefficients ( $d_{k,n}$ ).

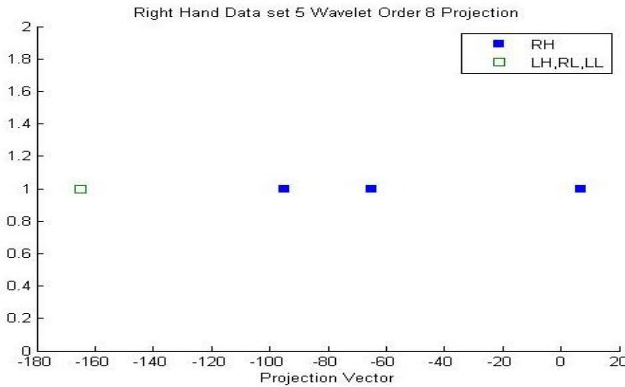


Fig. 6. Classification of right hand imagined movement

These wavelet filter coefficients were then processed with the Fisher Discriminant algorithm, in the same manner as were the linear predictor coefficients during the temporal classification procedure. This exercise was performed for a maximum scale factor of  $n=5$ . Four out of 16 dataset cases were misclassified by this method. This was evenly

distributed with 1 misclassification for each imagined movement.

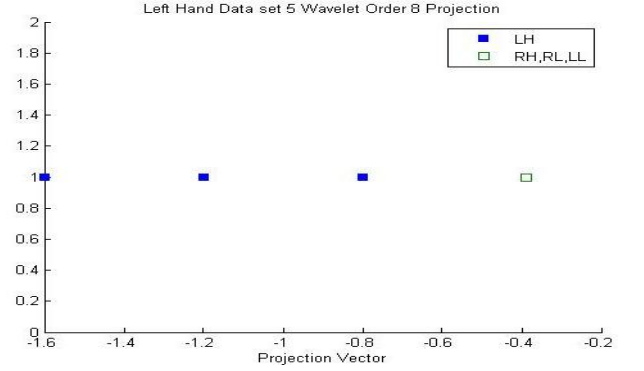


Fig. 7. Classification of left hand imagined movement

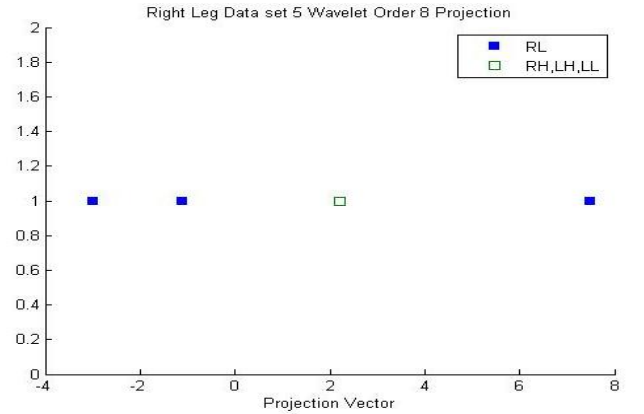


Fig. 8. Classification of right leg imagined movement

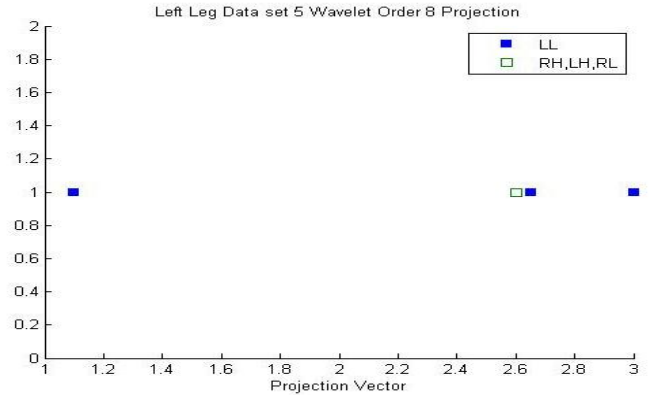


Fig. 9. Classification of left leg imagined movement

## II. RESULTS AND DISCUSSION

Recordings of the imagined-movement EEGs from an untrained subject were classified using different feature sets. With only 5 recorded data sets, a combination of three sets was used for feature extraction, the fourth for validation, and the 5<sup>th</sup> data set was used for performance verification of each developed classification method (testing).

Feature extraction in the time domain and frequency domain resulted in 100% class separation with the Fischer Linear Discriminant and compact intra-class clustering. The joint time-frequency domain feature extraction also demonstrated 100% correct classification rate. The wavelet decomposition feature extraction yielded a 75% success rate. Given our limited number of data points, a single misclassification resulted in a 25% error rate. The success of the presented classification schemes can also be attributed to the data set consistency, where all five data sets were recorded during a single session with a one-time electro-cap placement. The short time span of these recordings further limits the long-term EEG variability.

### III. CONCLUSION

The presented four approaches to EEG feature extraction demonstrated that each one of the four *a priori* known imagined tasks can be successfully classified.

Wavelet analysis has the ability to capture both temporal and spectral features. The use of different wavelet families may significantly improve classification performance. This should be the object of further exploration. Wavelets are families of oscillating functions whose energy is localized in time, making them well suited for feature extraction of non-stationary signals. Thus wavelet analysis should be a better candidate for on-line, real time BCI.

In order to develop a robust BCI, feature extraction and classifier training should utilize large data sets recorded over multiple sessions in different times. Given the changing dynamics of the brain and its underlying rhythms, a good BCI should have the ability to evaluate and adapt to the baseline affective-cognitive state of the subject (plasticity) without becoming unstable, a challenge that will be the subject of our future studies.

### ACKNOWLEDGEMENT

This work was supported in part by a grant from the University of Missouri's Research Board. We would like also to thank Mr. Andrew Castro for his help in conducting the recording sessions.

### REFERENCES

- [1] Karl, J.F. (2003), Characterizing Functional Asymmetries with Brain Mapping. *The Asymmetrical Brain*, edited by Keeneth Hugdahl and Richard J. Davidson. The MIT Press, 161-186.
- [2] Robert J.Z. (2003) Hemispheric Asymmetries in the Processing of Tonal Stimuli. *The Asymmetrical Brain*, edited by Keeneth Hugdahl and Richard J. Davidson. The MIT Press, 411-440.
- [3] Jean-Francois D., Guillanume T. 2002 Spatial and Temporal Dynamic of Phonological and Semantic Processes. *The Languages of the Brain*, edited by Ibert M.G., Stephen M.K., Yves C., Harvard University Press, 69-79
- [4] Clifford D., John J., Charles E., Herbert G. (2003). Complexities of Interhemispheric Communication in Sensorimotor Tasks Revealed by High-Density Event Related Potential Mapping. *The Asymmetrical Brain*, edited by Kenneth Hugdahl and Richard J. Davidson. The MIT Press, 341-408.
- [5] Stephen M.K. (2002). Einstein's Mental Images: The Role of Visual, Spatial, and Motoric Representations. *The Languages of the Brain*, edited by Albert M.G., Stephen M.K., Yves C., Harvard University Press, 271-287
- [6] James A.C., John J.B. (2003). The state and Trait Nature of Frontal EEG Asymmetry in Emotion. *The Asymmetrical Brain*, edited by Keeneth Hugdahl and Richard J. Davidson. The MIT Press, 411-440.
- [7] Wolpaw J. R., Birbaumer N., McFarland D. J., Pfurtscheller G., and Vaughan T. M. (2002) "Brain-computer interfaces for communication and control *Clinical Neurophysiology*, 113, pp 767-791.
- [8] Anderson, C. W., and Kirby, M. , (2003) "EEG Subspace Representations and Feature Selection for Brain-Computer Interfaces," *IEEE Conference on Computer Vision and Pattern Recognition*, vol. 5, no. 5, p. 51.
- [9] Jain, A.K., and Mao, J., (2000) "Statistical Pattern Recognition: A Review" *IEEE Transaction on Pattern Analysis and Machine Intelligence*, Vol. 22, No. 1.
- [10] Sornmo, L., Laguna, P. (2005) *Bioelectrical Signal Processing in Cardiac and Neurological Applications*. Burlington, MA USA: Elsevier Academic Press, pp. 286-312
- [11] Alpaydin, E. (2004). *Introduction to Machine Learning*. Cambridge, MA USA: The MIT Press.
- [12] Sarkar, T. K., Su, C., Adve, R., Salazar-Palma, M., Garcia-Castillo, L., & Boix, R. R. (1998, October). A Tutorial on Wavelets from an Electrical Engineering Perspective, Part 1: Discrete Wavelet Techniques. *IEEE Antennas and Propagation Magazine*, Vol. 40, No. 5, , p. 49-53.
- [13] Mathworks, Inc. (2007, September). *The Mathworks, Inc. Online Documentation, 2007b*. Retrieved 2006-2007, from Wavelet Toolbox Users Guide 4.1:<http://www.mathworks.com/access/helpdesk/help/toolbox/wavelet/>